Bulletin of the Seismological Society of America, Vol. 100, No. 1, pp. 384–391, February 2010, doi: 10.1785/0120090126

Short Note

Source Fault of the 2007 Chuetsu-oki, Japan, Earthquake

by Hiroe Miyake, Kazuki Koketsu, Kazuhito Hikima,* Masanao Shinohara, and Toshihiko Kanazawa

Abstract The 2007 Chuetsu-oki, Japan, earthquake is the world's first major earthquake upon a source fault that extends beneath a nuclear power plant and is also characterized by difficulty determining the source fault plane. Centroid Moment Tensor solutions indicate an M_w 6.6 reverse-faulting crustal earthquake with conjugate fault planes dipping to the northwest and southeast. Early results of aftershock locations suggest that either northwest-dipping plane or southeast-dipping plane can be the source fault plane of this earthquake. We carried out source inversions and empirical Green's function simulations of observed seismograms; however, they resulted in similar waveform residuals for the two fault planes. We then determined the relative locations of earthquake asperities to the hypocenter using travel-time differences of strong-motion pulses and relocated the aftershocks observed by ocean bottom seismometers deployed in the source region. These results imply that slips mainly occurred on the southeast-dipping fault plane. This implication was later confirmed by results of reflection surveys. During the earthquake, the Kashiwazaki-Kariwa nuclear power plant experienced stronger ground motions than those anticipated at the time of design. The ground motions consist of three seismic pulses that correspond to three asperities. The first and second pulses arose from rupture propagation to the plant, while the compact asperity on the distant southeast-dipping fault plane and its *S*-wave radiation pattern are responsible for the significant third pulse.

Introduction

The Chuetsu-oki earthquake occurred at 10:13 (Japan Standard Time [JST]) on 16 July 2007 in Niigata prefecture, along the west coast of Central Japan (Fig. 1a). The earthquake is characterized by difficulty determining the source fault plane from seismic, geodetic, and tsunami data. The Centroid Moment Tensor (CMT) solutions indicate that this earthquake is a reverse-faulting event with a moment magnitude of 6.6 and conjugate nodal planes dipping to the northwest and southeast. A source fault plane is usually identified from a distribution of aftershocks. As shown in Figure 1b, most of the aftershocks determined by the Japan Meteorological Agency (JMA) in the 12 hours following the earthquake occurred in an area located off the coast, southwest of the mainshock hypocenter. However, the three-dimensional (3D) aftershock distribution in Figure 1c shows not only a major trend dipping to the southeast but also a minor trend dipping to the northwest, so that we were unable to determine the source fault plane. In addition, the 2007 Chuetsu-oki earthquake occurred in the region connecting the Niigata-Kobe and Japan Sea Eastern Margin tectonic zones as shown in Figure 1a (Sagiya *et al.*, 2000; Earthquake Research Committee, 2003). The velocity structure in this region is so complex (e.g., Kato *et al.*, 2006) that it was difficult to determine the source fault planes of past events, such as the 2004 Chuetsu earthquake sequence (yellow star in Fig. 1b; e.g., Hikima and Koketsu, 2005) and the 1964 Niigata earthquake. In fact, for six months after the 2007 Chuetsu-oki earthquake, there was a controversy as to the location of the actual source fault.

Another significant feature of this earthquake was that the Kashiwazaki-Kariwa nuclear power plant (K-K plant in Fig. 1b) of the Tokyo Electric Power Company (TEPCO) is located in the source region. Seven reactors within the K-K plant experienced much stronger ground motions and longer periods than those anticipated at the time of plant design (TEPCO, 2007). The strong-motion seismographs installed on the base mats of seven reactors within the plant, as shown as KK1 to KK7 in Figure 2, were in fact the closest observational instruments to the earthquake. The observed ground accelerations are characterized by three seismic pulses

*Now at Seismic Design Group, R&D Center, Tokyo Electric Power Company, Inc.(TEPCO), 4-1, Egasaki-cho, Tsurumi-ku, Yokohama 230-8510, Japan.

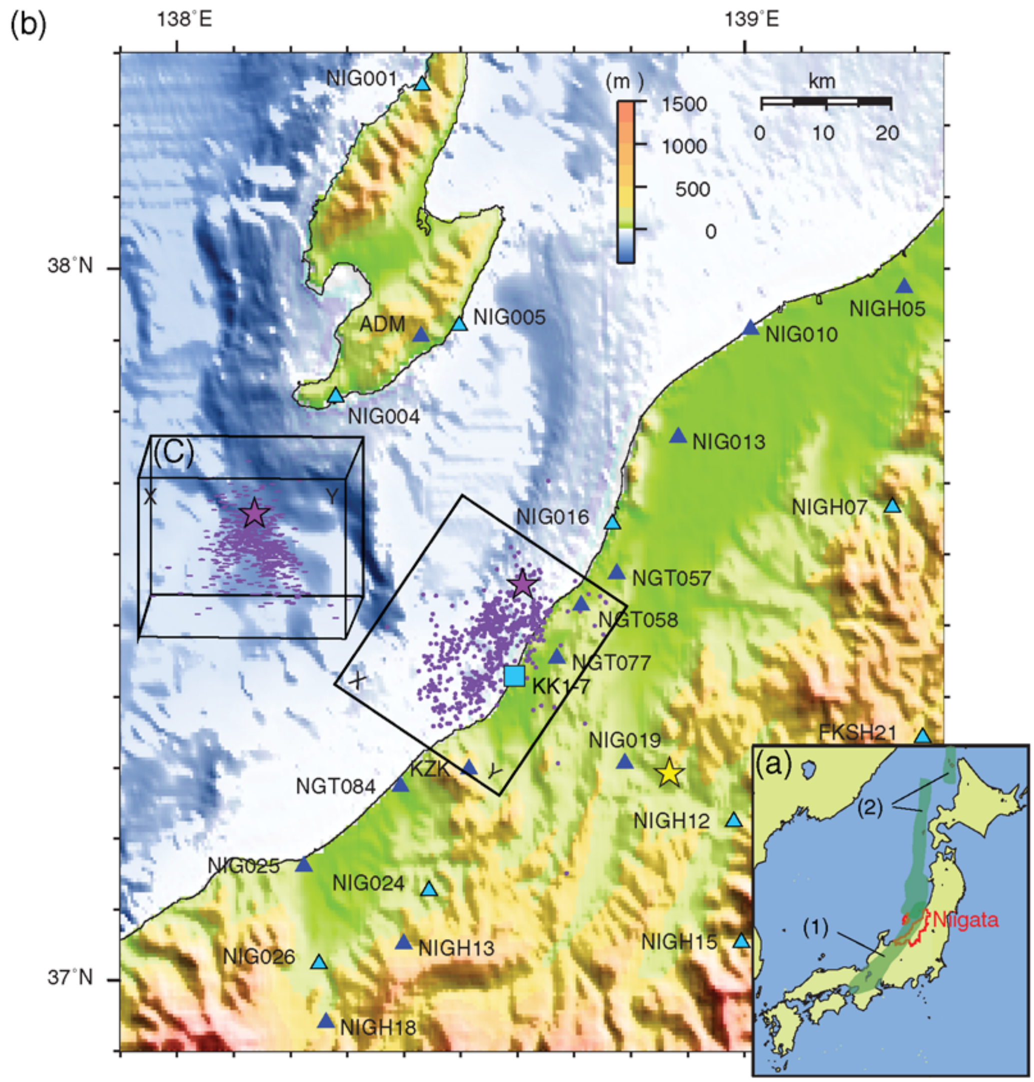

Figure 1. Geographic setting, distribution of the mainshock and aftershocks of the 2007 Chuetsu-oki earthquake, CMT solution, and the locations of seismograph stations. (a) Niigata prefecture is located near the connection between (1) the Niigata-Kobe and (2) Japan Sea Eastern Margin tectonic zones along the west coast of Central Japan. (b) Purple star, epicenters of the 2007 Chuetsu-oki earthquake; purple dots, aftershocks within 12 hours of the mainshock; yellow star, the 2004 Chuetsu earthquake, as determined by JMA; blue square indicates the location of the K-K plant, which houses seismographs KK1 to KK7; triangles, seismic stations whose records were used in this study. (c) 3D distribution of the mainshock and aftershocks within the area outlined by the black rectangle in (b).

indicated as pulses 1, 2, and 3 in Figure 2b. The peak ground acceleration of pulse 3 at KK1 is 680 cm/sec^2, which is 2.5 times greater than the design ground motion (TEPCO, 2007). Not only the peak ground accelerations but also the response spectra in Figure 2c are significantly over the design spectra in a broad period range. The periods of the dominant pulses are longer than the natural periods of safety-critical structures and facilities at the plant. However, the structures suffered only minor damage as a result of the ground accelerations (e.g., Cyranoski, 2007; Normile, 2007).

We investigate the reasons for these errors in risk assessment by analyzing the source fault of the 2007 Chuetsu-oki earthquake because such reasons are seismologically interesting and are important for the seismic safety of nuclear power plants as well. This analysis can lead to settlement of the controversy on the source fault.

Source Models

Four kinds of waveform analyses were performed for determining the source fault plane: point source analysis and finite source inversion of teleseismic records and finite source inversion and empirical Green's function simulation of strong-motion records. We first estimated the focal mechanism and hypocenter depth of the earthquake from the moment tensor inversion of teleseismic *P*-wave motions observed at 34 stations of the International Federation of Digital Seismograph Networks (FDSN). We confirmed that

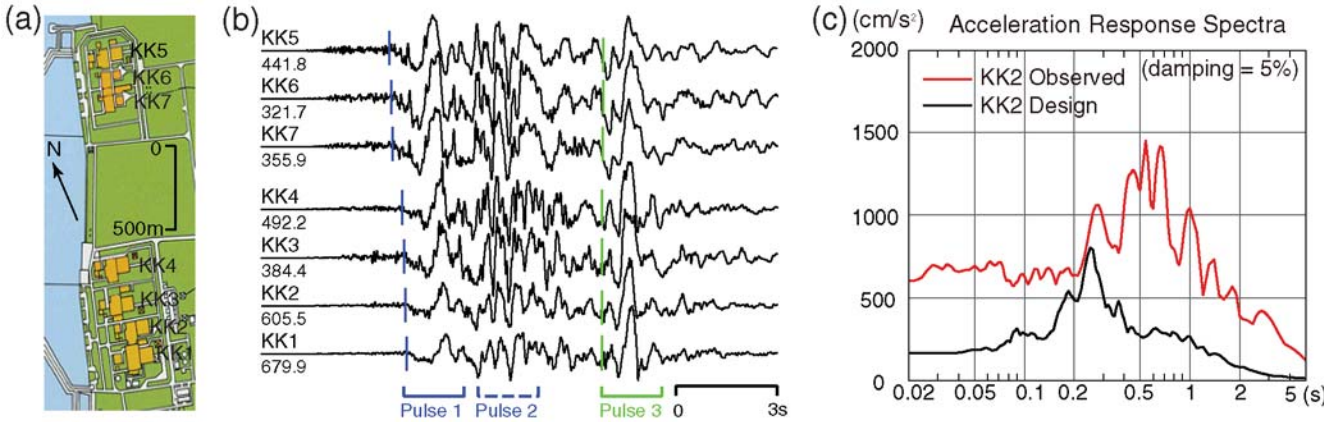

Figure 2. (a) Map of the K-K plant. The seismographs KK1 to KK7 are installed on the base mats of seven reactors aligned along the coast. (b) Sections of acceleration seismograms of the east–west component in cm/ sec^2 observed at the K-K plant during the mainshock. (c) Comparison of response spectra of the ground accelerations observed at KK2 (red) and assumed for KK2 at the time of plant design (black) (TEPCO, 2007). The response spectra were calculated with 5% damping.

the conjugate fault planes in the CMT solution were almost equivalent to the two trends identified in the distribution of aftershocks (Fig. 1c).

We then performed finite source inversions (Kikuchi *et al.*, 2003) of the previously described teleseismic records to determine the detailed geometry and depths of the conjugate fault planes. The best fit of synthetic to observed seismograms was accomplished with strikes/dips of 34°/36° and 214°/54° for the southeast- and northwest-dipping fault planes, respectively, though these teleseismic inversions for the two conjugate fault planes resulted in similar waveform residuals. We fixed the epicenter of 37.53824 N and 138.61744 E (Earthquake Research Institute, University of Tokyo; personal communication), and the hypocenter (point of rupture initiation) at a depth of 9 km resulted in the smallest degree of variance for the two conjugate fault planes. As the hypocenter is located close to the intersection of the two trends in the 3D aftershock distribution, we arranged two fault planes of 32 km in length by 24 km in width such that they intersect along a horizontal line at the hypocenter depth of 9 km (Fig. 3a). The upper terminating edges of the faults were confined to a depth beneath surficial sediments, and the northwest-dipping plane was not extended beyond the coast, as most of the onland vertical displacements were observed to be subsidence (Geographical Survey Institute, 2007).

To determine the detailed slip distribution on each conjugate plane, we carried out source inversions (Yoshida *et al.*, 1996) of strong-motion records observed at 12 of the stations plotted as the light blue square and triangles in Figure 1b. Considering the complex velocity structures in this area, we constructed an adaptive 1D model for each station in advance by inverting ground motion waveforms (Hikima and Koketsu, 2005) from an M_w 4.4 aftershock with a simple source mechanism (small red stars in Fig. 3b,c). Using the resulting velocity structure models, we obtained the slip distributions shown in Figure 3b,c for the southeast-dipping

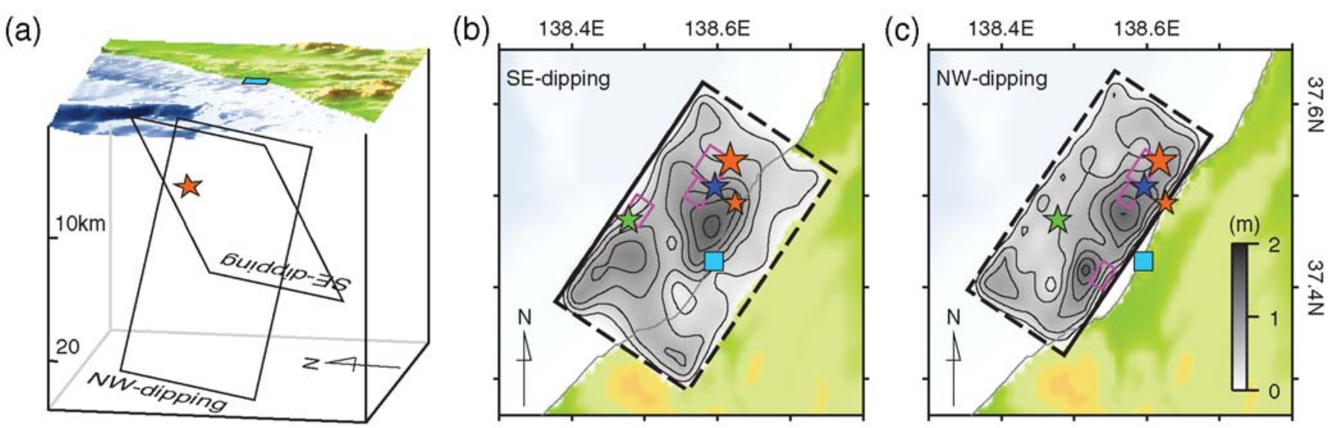

Figure 3. (a) 3D display of the southeast- and northwest-dipping fault planes, which intersect at the hypocenter depth of 9 km (red star). (b) Slip distribution recovered by strong-motion inversion for the southeast-dipping plane. Also shown: are the locations of the K-K plant (blue square), the epicenters of the mainshock and M_w 4.4 aftershock (red stars), and the first (blue star) and third (green star) asperities located by joint hypocenter determination. Pink rectangles represent the asperities identified by the empirical Green's function simulation. (c) As for (b) but for the northwest-dipping plane.

planes and northwest-dipping planes, respectively, from the source inversions of velocity seismograms filtered with a frequency band of 0.03 to 0.5 Hz. The main rupture propagates southwestward along strike with a speed of around 2.6 km/ sec; however, the inversions performed with the two conjugate planes yielded almost identical waveform residuals (Fig. 4), meaning that we were again unable to determine which plane was the source fault of the 2007 Chuetsu-oki earthquake. The seismic moments for the southeast- and northwest-dipping planes were respectively estimated to be 1.2×10^{19} N m and 1.4×10^{19} N m, which correspond to M_w 6.7.

The predominant frequencies of the seismograms observed at KK1 to KK7 are higher than the upper limit of the frequency band used in the strong-motion inversions, so that it is necessary to confirm the validity of our source model by simulating the broadband ground motions at the K-K plant. For this task, we employed the empirical Green's function method (Irikura, 1986), and again used the records of the M_w 4.4 aftershock with a frequency band of 0.2 to 10 Hz. We estimated the size and stress drop of the three asperities located close to the zones of large slip, as shown by pink rectangles in Figure 3b,c. The simulated seismograms on the two conjugate planes again show similar performance in comparison with the observed ground accelerations, velocities, and displacements at the K-K plant and other strong-motion stations (Fig. 5), as long as the high stress drop of 40 MPa is acceptable for the third asperity on the southeast-dipping plane, while the average stress drop is around 20 MPa. The overall waveform analyses previously described proposed that both the fault planes are possible.

Evidence Supporting the Southeast-Dipping Fault Plane

Additional support that the southeast-dipping fault plane is the source fault plane comes from (1) relocation of rupture starting points of asperities using strong-motion pulses, (2) aftershock observation by ocean-bottom seismometers (OBSs), and (3) reflection surveys in the source region.

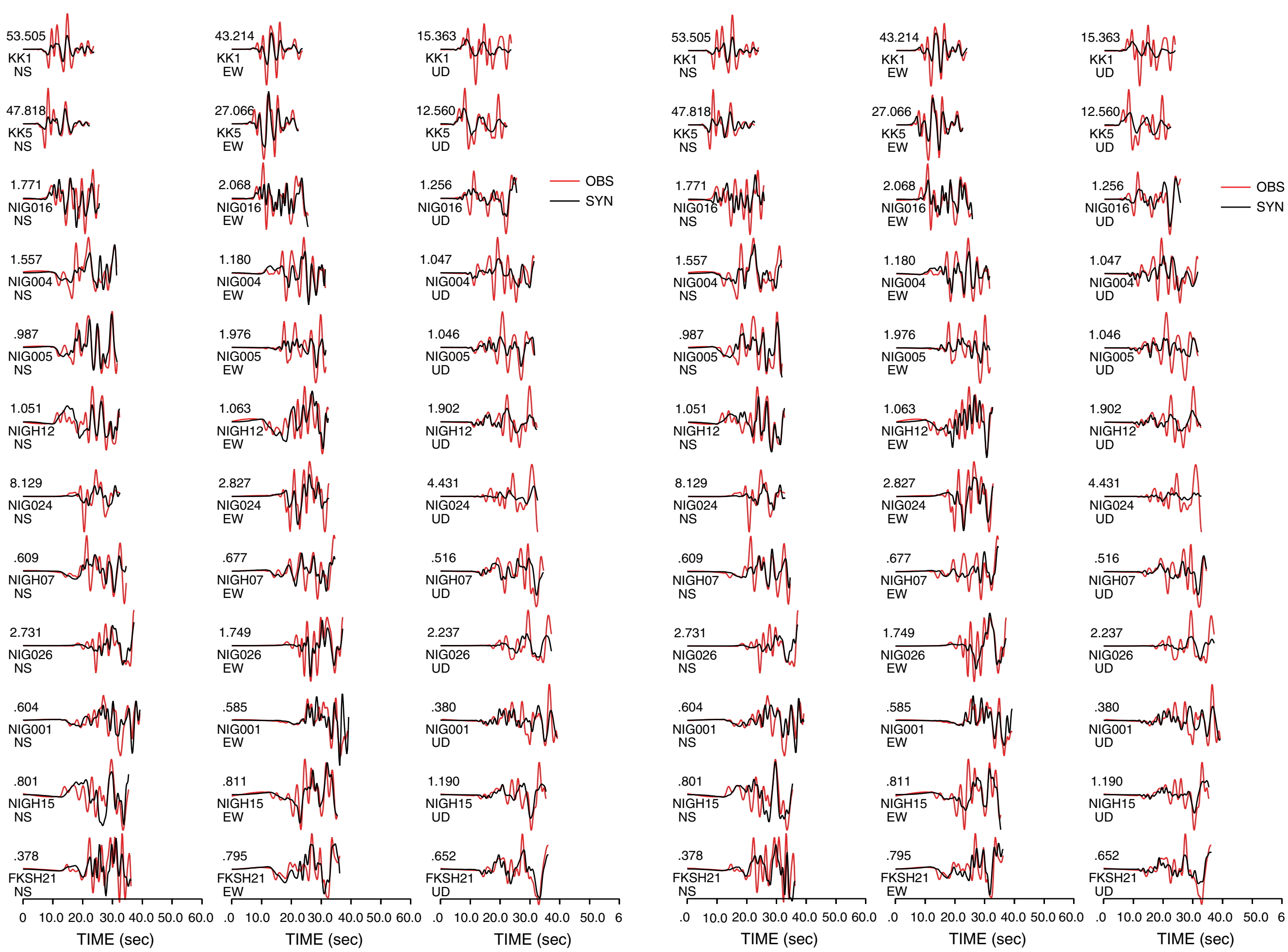

Figure 4. (Left) Comparison of observed (red) and synthetic (black) velocity seismograms in cm/ sec computed for the source inversion result on the southeast-dipping fault plane shown in Figure 3b. (Right) As in the left panel but for the northwest-dipping plane in Figure 3c. Stations are illustrated as the light blue square and triangles in Figure 1b.

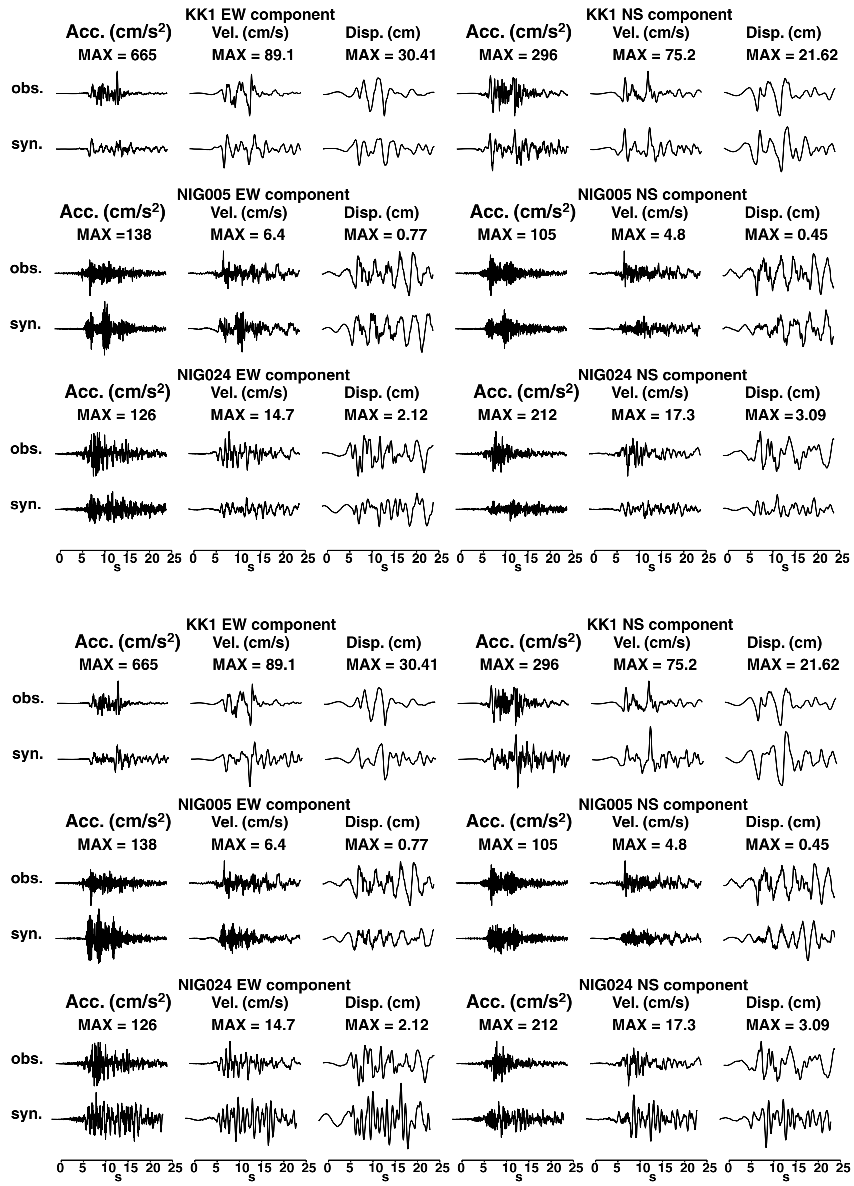

Figure 5. (Upper) Comparison of observed and synthetic seismograms computed for the empirical Green's function simulation result on the southeast-dipping fault plane shown in Figure 3b. (Lower) As in the upper panel but for the northwest-dipping plane in Figure 3c.

The first support comes from relocation of rupture starting points of asperities using strong-motion pulses. We aligned the seven seismograms observed at the K-K plant such that the initial *P*-wave arrivals matched the calculated travel times (Fig. 2b). We picked the arrivals of pulses 1 and 3 in Figure 2b at the positions indicated by the vertical blue and green bars, respectively. We then found that the arrival of pulse 1 was delayed in proportion to the distance of each reactor from the hypocenter. This finding indicates that the first asperity, corresponding to pulse 1, is located in a zone of large slip close to the hypocenters shown in Figure 3b,c. It is likely that this zone also includes the second asperity corresponding to pulse 2 because the distance between the first and second asperities is so small that the inversion of long-period seismograms cannot resolve the zone into separate asperities. In contrast to pulse 1, pulse 3 arrived at the seven reactors at similar times. This finding implies that the third asperity is independently related to small zones of large slip in the southern parts of the slip distributions shown in Figure 3b,c, as the reactors are located at approximately equal distances from each of the zones.

To further test these interpretations regarding the locations of the asperities associated with the seismic pulses, we picked the arrivals of the initial *P*-wave and pulse 1 on the seismograms recorded at 22 stations (including KK1 to KK7) in Figure 1b and determined the rupture starting point of the first asperity relative to the hypocenter. This joint hypocenter determination (Douglas, 1967) identified the

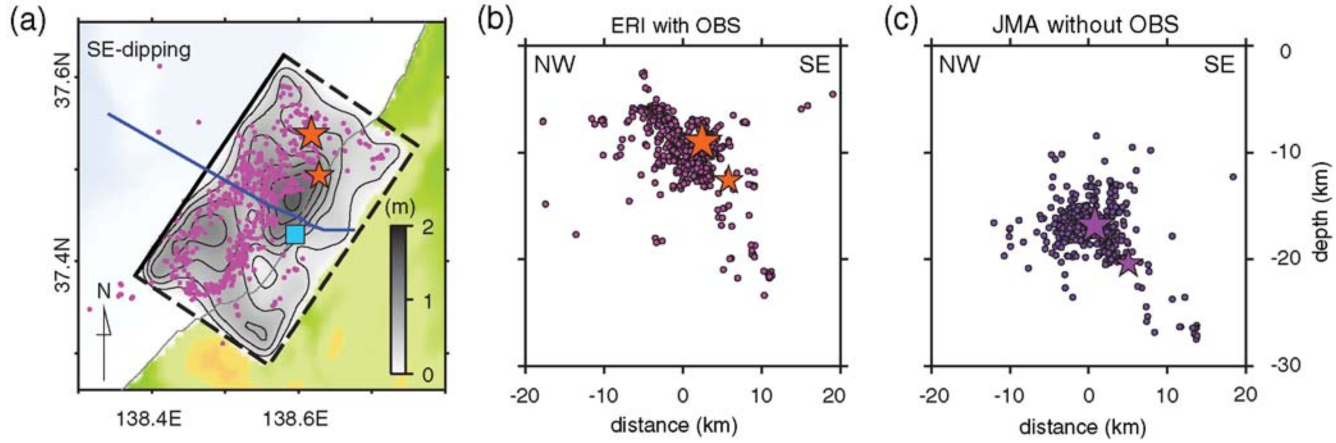

Figure 6. (a) Horizontal distribution of aftershocks relocated using OBS data by Shinohara *et al.* (2008) (pink dots). The slip distribution on the southeast-dipping fault plane (Fig. 3b) underlies the epicenters of the mainshock and M_w 4.4 aftershock relocated in this study (red stars) and the location of the K-K plant (blue square). The blue line indicates the reflection profile conducted by TEPCO (2008). (b) Their vertical distribution in the northwest–southeast cross section with the hypocenters of the relocated mainshock and M_w 4.4 aftershock (red stars). (c) Vertical distribution of aftershocks determined by JMA without OBS data during the same period (purple dots). Also shown are the locations of the mainshock and M_w 4.4 aftershock determined by JMA.

rupture starting point of the first asperity to be a short distance to the southeast of the hypocenter at a depth of 9 km with an error of within 1 km in depth, at a similar depth to that of the hypocenter. Therefore, the rupture starting point of the first asperity shown as the blue stars in Figure 3b,c can be located on both of the two conjugate planes, close to their line of intersection. The arrival of pulse 3 was only picked on the seismograms of KK1 to KK7, KZK, and ADM (Fig. 1b) because pulse 3 is contaminated by the long tail of pulse 2. The rupture starting point of the third asperity at a depth of 7.5 km with an error of within 1 km in depth was located at the position of the green stars to the west of the K-K plant in Figure 3b,c. Because there is no zone of large slip around the green star in Figure 3c, the third asperity should be located on the southeast-dipping plane as shown in Figure 3b.

The second support for the southeast-dipping fault plane is an aftershock distribution determined with OBS observations. Shinohara *et al.* (2008) deployed 32 OBSs in and around the earthquake source region from 25 July

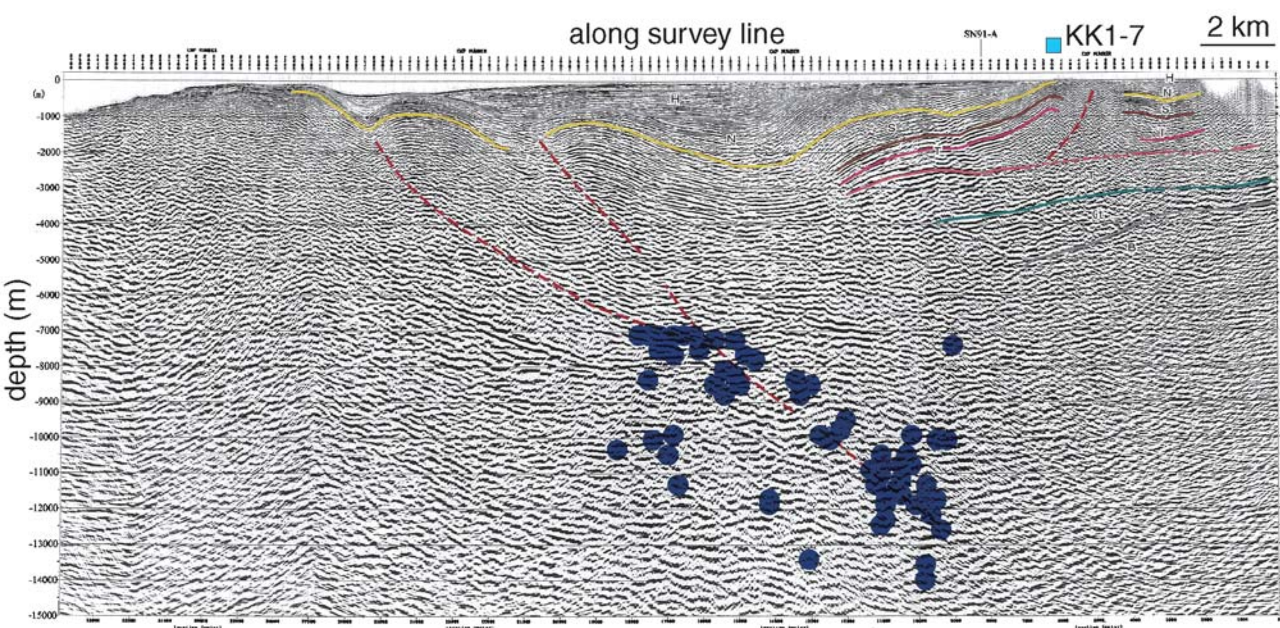

Figure 7. Reflection profile along a survey line in Figure 6 from the K-K plant to the northwest offshore (TEPCO, 2008). Colored lines indicate linearments identified by TEPCO (2008), among which the dashed ones were assumed to be related to the source fault plane of the 2007 Chuetsu-oki earthquake. Blue dots, aftershocks relocated using OBS data to the west of the K-K plant.

to 28 August 2007 to obtain an accurate aftershock distribution. The arrivals of direct *P*- and *S*-waves were picked from the seismograms recorded by the OBSs and onland stations, and then the aftershock hypocenters were precisely determined using the arrival times with the double-difference method (Waldhauser and Ellsworth, 2000), and the velocity structure model obtained through a seismic exploration in the same region. The relocated hypocenters obviously indicate that the southeast-dipping plane and few aftershocks occurred in the zones of large slip (Fig. 6a,b), though the hypocenters determined by JMA without OBS data during the same period still suggest the minor trend dipping to the northwest (Fig. 6c) as in Figure 1c. Mori (2008a) and Yukutake *et al.* (2008) also inferred the southeast-dipping plane from aftershock relocation using the land seismic network data.

The third support comes from reflection surveys performed after the earthquake by TEPCO (2008). Two surveys lines separated by about 20 km were deployed from the K-K plant to the northwest offshore along the fault width direction. The obtained seismic profile (Fig. 7) clearly shows southeast-dipping linearments to a depth of around 13 km. They coincide with the aftershocks relocated around the survey line and so should be related to the source fault of the 2007 Chuetsu-oki earthquake.

Conclusions

In summary, the most likely source model of the 2007 Chuetsu-oki earthquake consists of major slips on the southeast-dipping fault plane. The first and second asperities appear to be located near the intersection of the conjugate fault planes between the hypocenter and the K-K plant and the third asperity to the west of the K-K plant. The southeast-dipping plane is also supported by relocation of rupture starting points of asperities, aftershock relocation based on the OBS observations, and reflection surveys in the source region. Regarding the possibilities of minor slips on the northwest-dipping plane near the hypocenter, Takenaka *et al.* (2009) determined the initial rupture area, which is defined by the hypocenter and an early part of the first asperity, to be located on a northwest-dipping plane. Aftershocks relocated by Karo *et al.* (2008) aligned on both the northwest- and southeast-dipping fault planes. Nishimura *et al.* (2008) proposed a source fault consisting of a northwest-dipping plane for the northeast segment and a southeast-dipping plane for the southwest segment from Global Positioning System (GPS), Interferometric Synthetic Aperture Radar (InSAR), and leveling datasets; on the other hand, Mori (2008b) pointed out that the rate of aftershock activity for the 2007 Chuetsu-oki earthquake indicates a single planer fault pattern.

The asperities are recovered by both the source inversions and empirical Green's function simulations. This placement resulted in two large longer-period pulses at the K-K plant (pulses 1 and 2 in Fig. 2b) via the rupture directivity effect (Somerville, 2003; Koketsu and Miyake, 2008) mostly southwestward from the hypocenter to the K-K plant, as well as the hanging-wall effects pointed out by Cirella *et al.* (2008). The plant is not located in the forward rupture direction of the third pulse (pulse 3 in Fig. 2b), but it is possible that the maximum *S*-wave motion due to the radiation pattern can occur in the direction of the plant. Furthermore, the high stress drop within the third compact asperity is also able to generate such pulselike waves at the K-K plant. These are reasons for the underestimate at the time of plant design, though the primary reason should be considered as an oversight of the source fault of the 2007 Chuetsu-oki earthquake at that time.

Data and Resources

Seismograms and earthquake catalog were provided from the National Research Institute for Earth Science and Disaster Prevention (K-NET, KiK-net, F-net, and Hi-net), Japan Meteorological Agency, Tokyo Electric Power Company (TEPCO), Niigata prefectural government, and International Federation of Digital Seismograph Networks (FDSN). The TEPCO and FDSN data were obtained from the Association for Earthquake Disaster Prevention and the Incorporated Research Institutions for Seismology data management system, respectively. Relocated aftershocks were obtained from Shinohara *et al.* (2008).

Acknowledgments

We thank an anonymous reviewer and Michel Bouchon, associate editor of *Bulletin of the Seismological Society of America*, for constructive comments. This study was supported by a Grant-in-Aid for Special Purposes from Japan Society for the Promotion of Science (No. 19900003) and the Special Project for the Earthquake Disaster Mitigation in Tokyo Metropolitan Area from the Ministry of Education, Culture, Sports, Science, and Technology of Japan.

References

Cirella, A., A. Piatanesi, E. Tinti, and M. Cocco (2008). Rupture process of the 2007 Niigata-ken Chuetsu-oki earthquake by non-linear joint inversion of strong motion and GPS data, *Geophys. Res. Lett.* **35,** L16306, doi 10.1029/2008GL034756.

Cyranoski, D. (2007). Quake shuts world's largest nuclear plant, *Nature* **448,** 392–393.

Douglas, A. (1967). Joint epicentre determination, *Nature* **215,** 47–48.

Earthquake Research Committee (2003). Long-term evaluation of seismicity along the eastern margin of the Japan Sea, Headquarters for Earthquake Research Promotion, Tokyo, Japan, 35 pp. (in Japanese).

Geographical Survey Institute (2007). Abstract of the 174th Coordinating Committee for Earthquake Prediction Meeting, Geography and Crustal Dynamics Research Center, Geographical Survey Institute, Tsukuba, Japan: available at http://cais.gsi.go.jp/YOCHIREN/JIS/174/image174/010-012.pdf (in Japanese, last accessed May 2009).

Hikima, K., and K. Koketsu (2005). Rupture processes of the 2004 Chuetsu (mid-Niigata prefecture) earthquake, Japan: A series of events in a complex fault system, *Geophys. Res. Lett.* **32,** L18303, doi 10.1029/2005GL023588.

Irikura, K. (1986). Prediction of strong acceleration motions using empirical Green's function, in *Proc. of the 7th Japan Earthq. Eng. Symp.*, Tokyo, Japan, pp. 151–156.

Kato, A., S. Sakai, N. Hirata, E. Kurashimo, T. Iidaka, T. Iwasaki, and T. Kanazawa (2006). Imaging the seismic structure and stress field in the source region of the 2004 mid-Niigata Prefecture earthquake: Structural zones of weakness and seismogenic stress concentration by ductile flow, *J. Geophys. Res.* **111,** B08308, doi 10.1029/2005JB004016.

Kato, A., S. Sakai, E. Kurashimo, T. Igarashi, T. Iidaka, N. Hirata, T. Iwasaki, T. Kanazawa, and Group for the Aftershock Observations of the 2007 Niigataken Chuetsu-oki Earthquake (2008). Imaging heterogeneous velocity structures and complex aftershock distributions in the source region of the 2007 Niigataken Chuetsu-oki earthquake by a dense seismic observation, *Earth Planets Space* **60,** 1111–1116.

Kikuchi, M., M. Nakamura, and K. Yoshikawa (2003). Source rupture processes of the 1944 Tonankai earthquake and the 1945 Mikawa earthquake derived from low-gain seismograms, *Earth Planets Space* **55,** 159–172.

Koketsu, K., and H. Miyake (2008). A seismological overview of long-period ground motion, *J. Seismol.* **12,** 133–143.

Mori, J. (2008a). Determination of dip direction for the 2007 Chuetsu-oki earthquake from relocation of aftershocks using arrival times determined by cross-correlation, *Earth Planets Space* **60,** 1117–1120.

Mori, J. (2008b). Aftershock rates and spatial complexity for recent moderate earthquakes in Japan, Fall Meet. Suppl., Abstract S31C-08*Eos Trans. AGU* **89,** no. 53.

Nishimura, T., M. Tobita, H. Yarai, S. Ozawa, M. Murakami, T. Yutsudo, M. Ishimoto, T. Umesawa, T. Toyofuku, S. Kawamoto, T. Amagai, M. Fujiwara, A. Suzuki, S. Enya, T. Sasaki, M. Yokokawa, S. Oomori, S. Tanoue, H. Ikeda, M. Nemoto, H. Suito, F. Hayashi, H. Une, M. Koarai, and M. Tsuzawa (2008). Crustal deformation and a preliminary fault model of the 2007 Chuetsu-oki earthquake observed by GPS, InSAR, and leveling, *Earth Planets Space* **60,** 1093–1098.

Normile, D. (2007). Quake underscores shaky understanding of ground forces, *Science* **317,** 438–439.

Sagiya, T., S. Miyazaki, and T. Tada (2000). Continuous GPS array and present-day crustal deformation of Japan, *Pure Appl. Geophys.* **157,** 2303–2322.

Shinohara, M., T. Kanazawa, T. Yamada, K. Nakahigashi, S. Sakai, R. Hino, Y. Murai, A. Yamazaki, K. Obana, Y. Ito, K. Iwakiri, R. Miura, Y. Machida, K. Mochizuki, K. Uehira, M. Tahara, A. Kuwano, S. Amamiya, S. Kodaira, T. Takanami, Y. Kaneda, and T. Iwasaki (2008). Precise aftershock distribution of the 2007 Chuetsu-oki Earthquake obtained by using an ocean bottom seismometer network, *Earth Planets Space* **60,** 1121–1126.

Somerville, P. G. (2003). Magnitude scaling of the near fault rupture directivity pulse, *Phys. Earth Planet. In.* **137,** 201–212.

Takenaka, H., Y. Yamamoto, and H. Yamasaki (2009). Rupture process at the beginning of the 2007 Chuetsu-oki, Niigata, Japan, earthquake, *Earth Planets Space* **61,** 279–283.

Tokyo Electric Power Company (TEPCO) (2007). Report on the analysis of seismic observation data obtained at the Kashiwazaki-Kariwa nuclear power plant during the 2007 Chuetsu-oki earthquake (No. 1), http://www.tepco.co.jp/cc/press/betu07_j/images/070730d.pdf (in Japanese; last accessed May, 2009).

Tokyo Electric Power Company (TEPCO) (2008). Geology and geological structure at the Kashiwazaki-Kariwa nuclear power plant and vicinity: Results of additional investigations, http://www.tepco.co.jp/nu/material/files/g08072303.pdf (in Japanese; last accessed May, 2009).

Waldhauser, F., and W. L. Ellsworth (2000). A double-difference earthquake location algorithm: Method and application to the northern Hayward fault, *Bull. Seismol. Soc. Am.* **90,** 1353–1368.

Yoshida, S., K. Koketsu, B. Shibazaki, T. Sagiya, T. Kato, and Y. Yoshida (1996). Joint inversion of the near- and far-field waveforms and geodetic data for the rupture process of the 1995 Kobe earthquake, *J. Phys. Earth* **44,** 437–454.

Yukutake, Y., T. Takeda, and K. Obara (2008). Well-resolved hypocenter distribution using the double-difference relocation method in the region of the 2007 Chuetsu-oki Earthquake, *Earth Planets Space* **60,** 1105–1109.

Earthquake Research Institute
University of Tokyo
1-1-1 Yayoi, Bunkyo-ku
Tokyo 113-0032, Japan
hiroe@eri.u-tokyo.ac.jp

Manuscript received 25 May 2009